Biosensors and Bioelectronics 91 (2017) 262–267

Contents lists available at ScienceDirect

Biosensors and Bioelectronics

journal homepage: www.elsevier.com/locate/bios

# Kanamycin detection based on the catalytic ability enhancement of gold nanoparticles

Chengke Wang*, Dan Chen, Qingqing Wang, Rong Tan

*College of Food and Biological Engineering, Jiangsu University, Zhenjiang 212013, PR China*

ARTICLE INFO

*Keywords:*
Kanamycin
Gold nanoparticle
Catalytic ability
Colorimetric analysis
Biosensor

ABSTRACT

In this paper, we demonstrated that kanamycin could enhance the peroxidase-like activity of citrate-capped gold nanoparticles (AuNPs) through two steps: the attachment of kanamycin onto AuNPs through $-NH_2$ (on kanamycin) and −COOH (on AuNPs) interactions; and the specifically interaction between glucoside on kanamycin and AuNPs which changes the surface property of AuNPs, and produced •OH radicals and $Au^{3+}$ in the solution, and catalyzed the chromogenic reactions between 3, 3′, 5, 5′-tetramethylbenzidine (TMB) and $H_2O_2$. Based on this principle, a novel method for kanamycin detection has been developed. This method exhibited high sensitivity and selectivity, as low as 0.1 nM kanamycin could be detected with a linear range from 0.1 nM to 20 nM and 20nM to 300nM, respectively. This method was also successfully applied for the detection of kanamycin content in milk and meat samples.

## 1. Introduction

In recent years, on account of their unique optical, electronic, magnetic and biocompatibility characters, metal or alloy nanomaterials have aroused people's much attention, and are widely applied for biosensing (Bhattacharya and Mukherjee, 2008; Kumar et al., 2015; Bhattacharjee et al., 2016; Dutta et al., 2016), separation (Chen et al., 2016; Yildiz, 2016), imaging (McCarthy and Weissleder, 2008; Smith et al., 2008), drug delivery (Ghosh et al., 2008) and diagnostic application (Kim et al., 2016). Among these materials, the study and application of gold nanoparticles (AuNPs) has been of great interest (Kim et al., 2016; Nie et al., 2014). Its catalytic ability, namely peroxidase-mimetic property was also utilized by people in the biosensing assay (Wang et al., 2011b; Long et al., 2011; Zhu et al., 2013; Tao et al., 2013). However, the exact mechanism or process of these small Au species involved catalytic reactions are ambiguous or not consistent. The detected substances are also limited (*e.g.*, mainly include $Hg^{2+}$ that can form alloy with Au or molecules that can produce $H_2O_2$ in the presence of specific oxidase). Thus, it is urgent to explore the exact mechanism of AuNPs act as enzyme-like nanomaterials and it is desirable to develop a simple and inexpensive method for sensitively detecting more biological species, *e.g.*, harmful substances in the agricultural and food products that threaten people's health.

Antibiotics are widely used in the process of food production and livestock husbandry (Strachan and Davies, 2016; Tasho and Cho, 2016). However, due to its overuse, kanamycin residues in animal-derived food (*e.g.*, milk, meat and eggs) may lead to different degree of damage, including ototoxicity, nephrotoxicity and allergic reactions, et al. (Groschel et al., 2016; Liu et al., 2016). The European Union (EU) has established maximum residue limits (MRL) for kanamycin in edible tissues and milk: 200 nM for meat and 300 nM for milk (Song et al., 2011; Xing et al., 2015). So far, lots of analytical methods have been reported for detecting kanamycin, such as gas chromatograph (GC) (Preu et al., 1998), high performance liquid chromatography (HPLC) (Manyanga et al., 2010; Patel et al., 2015), liquid chromatography-mass spectrometry (LC-MS) (Oertel et al., 2004) and enzyme-linked immunosorbent assay (ELISA) (Chen et al., 2008; He et al., 2016; et al). Although these methods can efficiently detect kanamycin, there are still some hindrances, such as time-consuming, high cost, tedious and difficult operation, or are susceptible to interferences. Therefore, it is desirable and urgent to develop facile, cost-efficient and rapid assays for the detection of kanamycin with favorable sensitivity and selectivity.

Here, we found that kanamycin has the ability to enhance the catalytic ability of AuNPs by increasing the amounts of $Au^{3+}$ and •OH in the solution, which improve the oxidation degree of TMB in the presence of $H_2O_2$ and produced blue-colored species. This proposed method shows high selectivity and sensitivity, and can be used to detect kanamycin in milk, pork and chicken samples with satisfactory results.

* Corresponding author.
*E-mail address:* wangck@ujs.edu.cn (C. Wang).

http://dx.doi.org/10.1016/j.bios.2016.12.042
Received 6 October 2016; Received in revised form 6 December 2016; Accepted 16 December 2016
Available online 18 December 2016

## 2. Experimental section

### 2.1. Chemical and materials

$HAuCl_4 \cdot 4H_2O$ was purchased from Sigma-Aldrich (St. Louis, MO). Antibiotics (kanamycin sulfate, streptomycin sulfate, neomycin sulfate, sisomicin sulfate, tobramycin sulfate, ribostamycin sulfate and spectinomycin sulfate) and TMB were obtained from Aladdin Reagent Co., Ltd. (Shanghai, China). Aptamer with the following sequence: 5′-TGGGG GTTGA GGCTA AGCCG A-3′ was chosen according to the previous report (Wang et al., 2016) and obtained from Sangon Biotechnology Co. Ltd. (Shanghai, China)·$H_2O_2$, NaCl, trisodium citrate dihydrate, acetic acid, cystamine, Tris-hydroxymethyl aminomethane (Tris), dimethyl pyridine N-oxide (DMPO) and HCl were acquired from Sinopharm Group Chemical Reagent Co., Ltd. (Shanghai, China). Glucose, maltose, lactose, fructose, sucrose, sodium gluconate, gluconolactone, N-methyl-D-glucamine, β-D-glucose pentaacetate, β-D-glucosamine pentaacetate, N-acetyl-D-glucosamine, D-glucosamine hydrochloride were acquired from Shanghai Titan Scientific Co., Ltd (Shanghai, China). The milk, pork and chicken samples were acquired from a local supermarket. All other chemicals were of analytical grade and used without further purification. Double distilled water (dd $H_2O$) was used throughout the experiment.

### 2.2. Apparatus

The UV–visible (UV–vis) absorption spectra were recorded on a Tecan Infinite 200 PRO microplate reader (Mannedorf, Swiss). The Fourier transform infrared (FTIR) spectra (4000–650 $cm^{-1}$) were recorded with a Nicolet IS10 FTIR spectrometer (Thermo Fisher Co., Ltd., USA). pH values of the solutions were adjusted using a Leici PHS-3E pH meter (INESA Scientific Instrument Co., Ltd., China). The centrifugation process was operated using a CF-10 centrifuge (WiseSpin Co., Ltd., Korea). All measurements were carried out at room temperature otherwise mentioned specially.

### 2.3. Synthesis of AuNPs

13 nm AuNPs were prepared by reducing $HAuCl_4$ with trisodium citrate according to the previous report (Wang et al., 2011a, 2010b). The concentration of AuNPs was determined by UV–vis spectroscopy as 6.7 nM (the molar extinction coefficient is $2.7\times10^8$ $M^{-1}$ $cm^{-1}$ at 518 nm (Demers et al., 2000).

### 2.4. Detection of kanamycin in aqueous solutions

10 μL different concentrations of kanamycin, 50 μL Tris-HCl buffer (25 mM), 120 μL dd$H_2O$ and 20 μL AuNPs were added into 96 wells plate successively. After mixed thoroughly and reacted for 10 min, a mixture of 50 μL Tris-HCl (25 mM), 25 μL TMB (6.7 mM) and 25 μL $H_2O_2$ (2 M) were added into the wells, after reacted for 45 min, the UV–vis absorption spectra of the final solutions were recorded from 500 to 800 nM.

### 2.5. X-ray photoelectron spectroscopy (XPS) measurement

XPS spectra were collected using a Thermo ESCALAB250 X-ray photoelectron spectroscope (Thermo, UK). AuNPs solutions in the absence and presence of kanamycin were dropped on a Si substrate and oven-dried before measurement.

### 2.6. Electron paramagnetic resonance (EPR) measurement

EPR signal was measured by a Bruker ESP 300E spectrometer (Bruker, Rheinstetten, Germany) with microwave bridge (receiver gain, $1\times10^5$; modulation amplitude, 2 Gauss; microwave power, 10 mW; modulation frequency, 100 kHz). A sample containing 0.1 M DMPO was transferred to a quartz capillary tube and placed in the EPR cavity. Under the UV-irradiation at 355 nm, EPR signal was detected using DMPO as the spin trap.

### 2.7. Real samples pretreatment and detection

Different amounts of kanamycin were added into 10 mL milk samples, then 20% (v/v) acetic acid was added gradually until the pH of the solution reached 4.5, after the solutions were centrifuged at 13,200 r/min for 15 min, the supernatant was pipetted and filtrated using a 0.22 μm membrane, the filtrate was collected. The fat and other organs were removed from 5g pork or chicken, and then the meats were shattered sufficiently using surgical scissors. After adding 8 mL Tris-HCl buffer (pH 7.5, 25 mM) and mixed thoroughly for 5 min, the mixtures were centrifuged at 3000 r/min for 20 min, then different amounts of kanamycin were added into the supernatant. The solutions acquired by pretreating milk, pork and chicken were detected using our developed method.

## 3. Results and discussions

### 3.1. AuNPs as peroxidases for detecting kanamycin

According to previous reports, TMB can be oxidized by $H_2O_2$ and produce a blue color product with a significant maximum absorbance at 650 nm (Wang et al., 2015), as shown in Fig. S1. After adding AuNPs into the TMB-$H_2O_2$ solution, the reaction of TMB and $H_2O_2$ can be catalyzed by citrate-capped AuNPs, with further addition of kanamycin, the catalytic activity of AuNPs was further improved, and the color of the mixture was also changed to deep blue, enabling the colorimetric determine the concentration of kanamycin in solutions.

### 3.2. Optimization of detecting conditions

In order to select the optimal experimental conditions for detecting kanamycin, the pH value of the solution, the amounts of TMB and $H_2O_2$ and the reaction time were carefully studied. As shown in Fig. 1A and S2, while varying the pH of the solution from 4 to 7.5, the color intensity and the absorbance of the mixture increased no matter there is kanamycin or not, the optical densities (OD) at maximum absorbance wavelength of 650 nm ($OD_{650}$) were also increased consequently. $\Delta OD_{650}$ ($OD_{kanamycin}-OD_0$) was used as a criterion to optimize the detection conditions, where the $OD_{kanamycin}$ and $OD_0$ is the $OD_{650}$ of the solutions in the presence and absence of kanamycin, respectively. The $\Delta OD_{650}$ was increased until pH value was 7.5. this may because that TMB-$H_2O_2$ chromogenic reaction would be inhibited at lower pH (Li et al., 2009); on the other hand, higher pH value may facilitate the interaction between kanamycin and AuNPs by the electrostatic interactions. Nevertheless, under much higher pH condition, $H_2O_2$ becomes unstable and tends to decompose into $H_2O$ and $O_2$ (Wang et al., 2010c). Therefore, pH 7.5 was chosen in the following experiment.

The amounts of TMB and $H_2O_2$ are of great importance in the TMB-$H_2O_2$ chromogenic system, as shown in Fig. 1B and S3, with increasing the amounts of TMB and $H_2O_2$ simultaneously, the color intensity and the absorbance of the solution is increased consequently, the $OD_{650}$ of the solution was also increased significantly. When the final concentrations of TMB and $H_2O_2$ are 0.56 mM and 0.17 M (*i.e.*, 25 μL TMB and 25 μL $H_2O_2$ in the solutions), the $\Delta OD_{650}$ was highest, if the concentrations still increased, the background signal in the absence of kanamycin is too high, which results in the $\Delta OD_{650}$ decreased, consequently (Li et al., 2009). Therefore, 0.56 mM TMB and 0.17 M $H_2O_2$ were used in the following experiment. The reaction time after adding TMB and $H_2O_2$ into the solution was also investigated, as shown in Fig. 1C, and the $\Delta OD_{650}$ increased with increasing the reaction time from 0 to 45 min, and kept constant after 45 min. So,

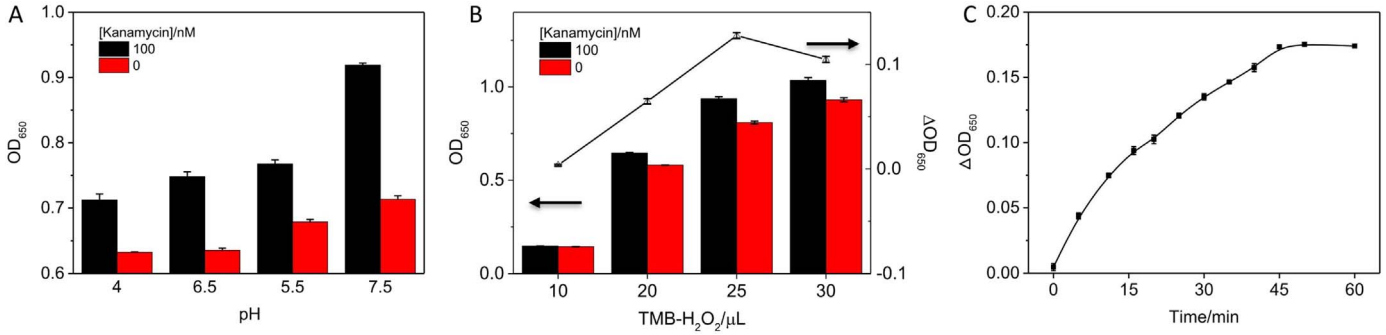


**Fig. 1.** The experiments for determining the optimal detection conditions. The optical density at 650 nm ($OD_{650}$) of UV–vis absorption spectra of TMB-$H_2O_2$ and AuNPs solutions at different pH in the absence and presence of kanamycin (A), the $OD_{650}$ and $\Delta OD_{650}$ (the differences between the $OD_{650}$ in the presence and absence of kanamycin) changes of UV–vis absorption spectra of AuNPs solutions with the addition of different amounts of TMB and $H_2O_2$ before and after the addition of kanamycin (B) and the $\Delta OD_{650}$ changes of the TMB-$H_2O_2$ and AuNPs solutions as a function of interaction time in the presence of kanamycin (C), respectively. The error bars represent the relative standard deviation of three experimental results. The concentrations of AuNPs and kanamycin are 0.67 nM and 100 nM, respectively.

the optimal reaction time was determined as 45 min.

### 3.3. Detection of kanamycin based on AuNPs

Under the optimal conditions, solutions with different concentrations of kanamycin were detected using above mentioned colorimetric method. As shown in Fig. 2 and S4, the color intensity and the absorbance of TMB-$H_2O_2$ and AuNPs solutions were increased with increasing the concentration of kanamycin from 0 nM to 1000 nM, and the $OD_{650}$ of the solutions was also lineally increased with the concentration of kanamycin increasing from 0.1 to 100 nM (the calibration curve is $OD_{650}=0.7846+0.00134C_{kanamycin}$), the limit of detection (LOD) is 0.1 nM (3 times of standard deviation of the blank, 3σ), which is equal to or better than that of many other reported assays (see Table S1) and is far below the MRL in food products. Inset of Fig. 2B shows the color of the mixtures changed from light blue to deep blue when the concentration of kanamycin increased from 0 to 1000 nM, which is convenient for the semi-quantitatively determine kanamycin by naked eyes. The $OD_{650}$ began to saturate after 500 nM, this may because that the number of kanamycin attached onto the AuNPs or the catalytic ability of AuNPs reached saturate, the study of exact mechanism is under progress.

### 3.4. Selectivity and kinetics of AuNPs based assay

The selectivity is essential for a successful method for detecting kanamycin. In this AuNPs based colorimetric method, we assumed that the kanamycin detection was based on the selective interaction of AuNPs with kanamycin. In order to verify the specificity of the assay, the interferences of other 6 kinds of antibiotics on the kanamycin detection were also studied. As shown in Fig. 3A and S5, the $OD_{650}$ of the solution after adding kanamycin was much higher than other species, this experimental result indicates that our method has satisfactory selectivity towards kanamycin.

The kinetics of AuNPs based assay was also investigated. As shown in Figs. S6, the $OD_{650}$ changes of solutions in the presence of 100 nM kanamycin are faster than the solutions in the absence of kanamycin, according to the simulated curves, the first-order kinetic constants increased from $1.78\times10^{-2}$ $min^{-1}$ to $2.31\times10^{-2}$ $min^{-1}$ when 100 nM kanamycin was employed, which also demonstrate the catalytic abilities enhancement of AuNPs by kanamycin. The phenomenon may originate from the produced compounds (*e.g.*, redox-active species, *vide infra*) by the interaction of kanamycin with AuNPs. The exact theoretical model and details of the interactions will be investigated in the future work.

### 3.5. The mechanism of AuNPs based assay

In order to further illustrate the details of interaction between kanamycin and AuNPs, and to investigate the mechanism of AuNPs based colorimetric assay, some additional experiments were carried out. In fact, the kanamycin stimulated peroxidase mimetic activity of AuNPs can also be visually observed through the decomposition of $H_2O_2$ even if without TMB. As shown in Fig. S7, after the addition of

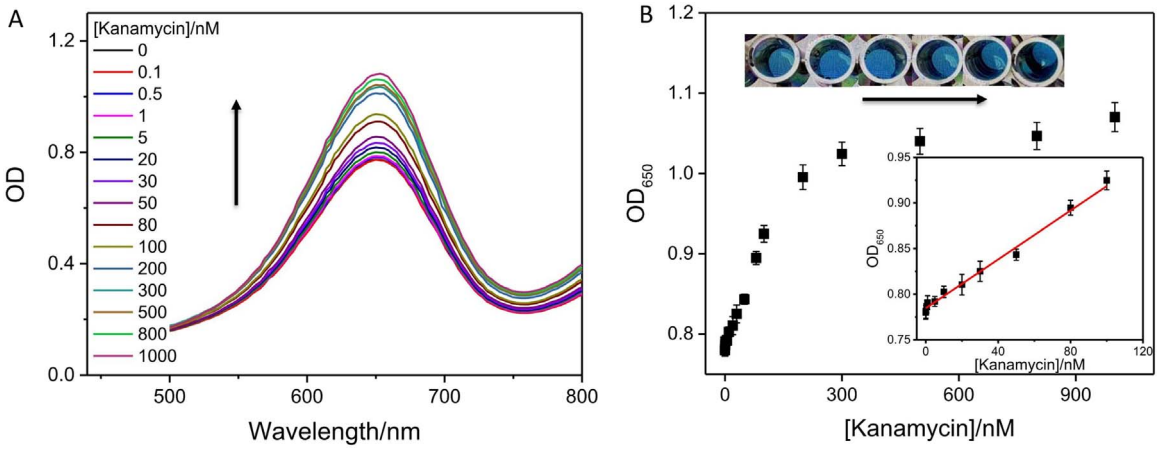


**Fig. 2.** The colorimetric method for detecting kanamycin. The UV–vis absorption spectra of TMB-$H_2O_2$ and AuNPs solutions in the presence of different concentrations of kanamycin (A) and the $OD_{650}$ changes of the solutions as a function of kanamycin concentration (B), respectively. Inset of (B) indicate the corresponding images of solutions in the presence of 0, 0.1, 1, 10, 100 and 1000 nM kanamycin (from left to right), respectively. The error bars represent the relative standard deviation of three experimental results. The concentrations of TMB, $H_2O_2$ and AuNPs, are 0.56 mM, 0.17 M and 0.67 nM, respectively.

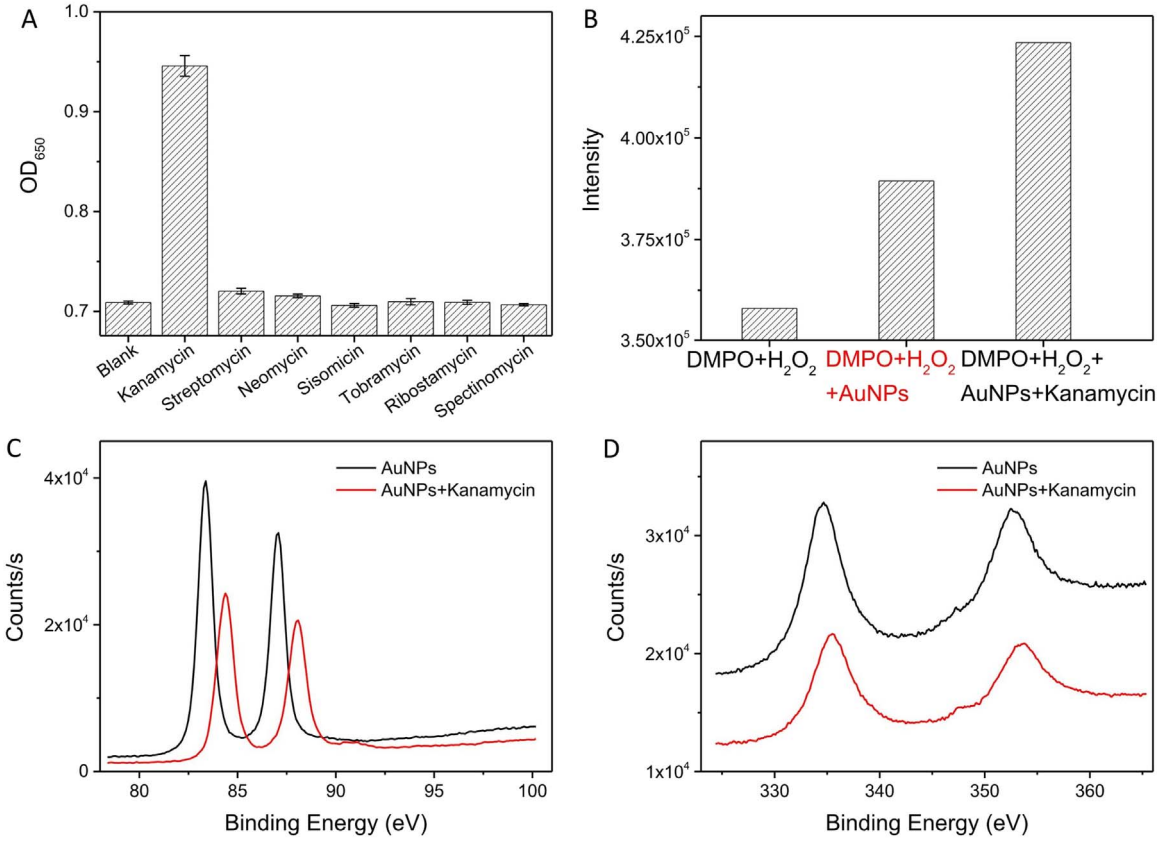


**Fig. 3.** The selectivity, EPR and XPS experiment. The $OD_{650}$ of the TMB-$H_2O_2$ and AuNPs solutions in the presence of different kinds of antibiotics (A), the EPR signals at 3502 G of the solutions contained DMPO, $H_2O_2$, AuNPs and kanamycin, respectively (B). The Au 4 f (C) and Au 4d (D) XPS spectra of the AuNPs in the absence and presence of kanamycine. The error bars represent the relative standard deviation of three experimental results. The concentrations of DMPO, AuNPs, $H_2O_2$ and kanamycin are 0.1 M. 0.67 nM, 2 M and 200 nM, respectively.

kanamycin into the mixture of AuNPs and $H_2O_2$, lots of bubbles were produced in the solutions; on the contrary, the solutions in the absence of kanamycin or presence of other antibiotics didn't produce lots of bubbles, indicating the kanamycin-AuNPs accelerated decomposition of $H_2O_2$ just like natural peroxidases, this experimental results are agreement with previous report and the selectivity experimental results (Long et al., 2011).

In addition to the bubble-producing experiment that can be seen by naked eyes, this kanamycin-stimulated peroxidase-like activity can be further identified by measuring the hydroxyl radical (•OH) with EPR measurement, using DMPO as the spin trap. As shown in Fig. 3B and S8, after adding $H_2O_2$ into the DMPO solution, the EPR signal intensity increased significantly, which indicated that lots of •OH radicals were produced in the solution and trapped by DMPO, the signal intensity of •OH radicals generated by ultraviolet irradiation of $H_2O_2$ increased with the addition of AuNPs, which is a typical behavior of peroxidase (Wang et al., 2011b). In the presence of kanamycin, the EPR signal intensity further increased. This result also manifests that kanamycin can enhance the peroxidase-like activity of AuNPs by increasing the formation of •OH radicals in solutions, which is agreement with previous report (Zhu et al., 2013).

As reported by Zheng and Huang (Long et al., 2011; Zhu et al., 2013), the catalytic ability of Au cluster has a close relationship with the valence changes (*i.e.*, $Au^0$, $Au^+$, $Au^{3+}$) of Au on the surface. Any compounds that binding onto Au would change the surface behavior of Au spheres, and interfering the catalytic activity of AuNPs or Au clusters. Hence, XPS experiment was used to investigate the valence changes of Au and demonstrate the supposition. As shown in Figs. 3C, 3D and S9, it was revealed that there was mainly $Au^0$ in the solution in the absence of kanamycin. However, after the addition of kanamycin, the full width at half maximum (FWHM) and peak area clearly changed; especially, the peak position of Au moved to a higher binding energy, which is in the typical energy region of $Au^{3+}$. All these results demonstrated that kanamycin can interact with AuNPs and change the binding energy of Au, and released lots of $Au^{3+}$ which may act as oxidizing agent to oxidize the TMB, and to further enhance the catalytic activity of AuNPs (Zhu et al., 2013).

Does the gold ions indeed play an important role in this detecting process? Next, $HAuCl_4$ was used to verify $Au^{3+}$ has the ability to catalyze TMB and form chromogenic species, as shown in Fig. S1, the absorbance of the solution was dramatically increased after adding $HAuCl_4$ into TMB-$H_2O_2$ systems, even there is no AuNPs and kanamycin, this result indicated that the production of $Au^{3+}$ as a result of the interaction between kanamycin and AuNPs plays a crucial role in the catalytic ability enhancement of AuNPs.

In order to further find out the steps that involved in the interactions between kanamycin and AuNPs, aptamer was used to specially interact with kanamycin, as shown in Fig. S10, the kanamycin can induce the UV–vis spectra of AuNPs red-shifted, this may because that trisodium citrate reduced AuNPs contain lots of negative citrate ions, and are negative-charged (Li et al., 2014), while kanamycin is positive-charged, the electrostatic force makes kanamycin approached to AuNPs, and the surface charge of AuNPs was neutralized, which leads to the assembly of AuNPs. However, after the addition of aptamer, as aptamer can strongly and specially interact with kanamycin, and results in the desorption of kanamycin from AuNPs (Wang et al., 2016), the spectrum of AuNPs solution was recovered, and the color of the solutions is also changed from purple to red, consequently. These experimental results indicated that the kanamycin was firstly attached onto the AuNPs, and this process is reversible.

As in this assay, AuNPs was reduced and stabilized by citrate, we may speculate that citrate ions on the surface of AuNPs play an

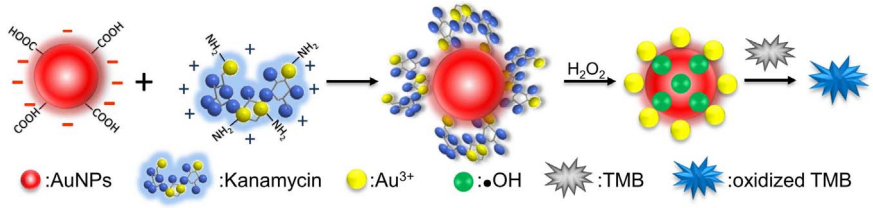


**Scheme 1.** Schematic illustration of the AuNPs based colorimetric method for detecting kanamycin. The illustration is not drawn to scale.

important role in the interaction between kanamycin and AuNPs. As shown in Fig. S11, after centrifuged sufficiently to remove the surrounding medium and dispersed in $H_2O$, citrate on the AuNPs was diminished. After the addition of TMB and $H_2O_2$, compared with citrate-capped AuNPs system, the color intensity of the solutions decreased as well, no matter there is kanamycin or not. On the other hand, when NaCl was added into the AuNPs solutions, as NaCl is able to significantly make AuNPs aggregated by charge shielding effect, and this process is irreversible even if aptamer was added afterwards (Wang et al., 2010a, 2016) (data is not shown here). The aggregated AuNPs show relatively low catalytic ability. These experimental results revealed that kanamycin was attached onto AuNPs by interacting with the citrate ions, and if they were removed, the catalytic ability of AuNPs were decreased dramatically. Besides, AuNPs can be stabilized by citrate ions, the removing of these ions would decrease the stability of AuNPs and inhibit the interaction of AuNPs with TMB-$H_2O_2$ system (*i.e.*, by electrostatic interaction between negative charged AuNPs and positive charged TMB). In general, as the NaCl induced small AuNPs aggregated to large species, the surface area was decreased significantly (Demers et al., 2000), and the citrate ions that involved in the catalytic reaction were also decreased, consequently. Therefore, the decrease of catalytic activity of AuNPs may originated from two aspects: the citrate ions were diminished by removing (*e.g.*, centrifugation) or embedding (*e.g.*, citrate ions in the large AuNPs aggregates); and the active reaction center was diminished (*e.g.*, small AuNPs formed large aggregates or Au cluster turned to large dimension substances (Demers et al., 2000)).

Next, the group of kanamycin that directly interact with AuNPs was explored. Kanamycin was firstly interacting with acetic acid in order to react with $-NH_2$, as shown in Fig. S12, after pretreated with acetic acid, the acetic acid-kanamycin compound shows relatively low catalytic enhancement capacity, even high concentration (500 nM) of kanamycin was added, the color and the $OD_{650}$ of the mixtures are not changed a lot either. Further study was carried out by replacing kanamycin with other 12 kinds of species including different kinds of saccharide and glucose derivatives, as shown in Fig. S13, there was only kanamycin that has the catalytic ability to produce an enhanced signal, considering these substitutes contain less or no $-NH_2$, combined with the results of acetic acid masking experiment, we may demonstrate that the four $-NH_2$ groups in the kanamycin is of particularly importance for the interaction between kanamycin and AuNPs, and it is the interaction of $-NH_2$ on kanamycin and –COOH on citrate that realized the specific recognition of kanamycin by AuNPs.

Cystamine was also used as substitute of kanamycin to explore the role of glucoside section in the kanamycin-AuNPs catalytic system. As shown in Fig. S12, compared with kanamycin, the cystamine has much lower possibility to change the peroxidase mimetic property of AuNPs. This result indicated that after kanamycin attached onto the AuNPs using $-NH_2$, the glucoside further interacts with AuNPs, and changes the surface property of AuNPs, which finally induced the catalytic ability enhancement of AuNPs.

### 3.6. FTIR experiment

FTIR is a suitable approach to study the interaction modes of different molecules, especially the changes on the surfaces of each compounds. In order to investigate the changes of functional groups during the interactions between compounds and AuNPs, the FTIR spectra of four representative compounds (neomycin, ribostamycin, tobramycin and kanamycin) were recorded in the absence and presence of AuNPs. As shown in Fig. S14, the spectra are not changed a lot for neomycin, ribostamycin and tobramycin after the addition of AuNPs, this indicated that these molecules are not attached onto AuNPs or there were no additional reactions between them, this may explain that these compounds have no ability to enhance the catalytic property of AuNPs and is consistent with our selectivity experimental results. On the contrary, after interact with AuNPs, the FTIR spectra of kanamycin between 2800 $cm^{-1}$–3500 $cm^{-1}$ and 1300–1700 $cm^{-1}$ wavenumbers were changed significantly, which could be ascribe to the diminish of N-H stretch (3100–3500 $cm^{-1}$), O-H stretch (3200–3500 $cm^{-1}$) and O-H vibration (1300–1500 $cm^{-1}$) on kanamycin, and the increase of -COOH (2500–3400 $cm^{-1}$) on AuNPs and C-N of amide groups (1400–1420 $cm^{-1}$) (Burns and Ciurczak, 2008; Lin-Vien et al., 1991), and is originated from the interaction between kanamycin and AuNPs. As these antibiotics have no ability to enhance the catalytic activity of AuNPs, although they all contained $-NH_2$ and glucoside sections, we may assume that these different compounds may have different steric configurations, the steric hindrance of these species when they interact with AuNPs made them inaccessible to AuNPs or unable to change the surface property of AuNPs, the exact mechanism need to further theoretical simulation, this work will be considered in our following experimental schedules.

In summary, based on the above mentioned experimental results, we may propose the model for the course and mechanism of kanamycin initiated catalytic activity enhancement of AuNPs. As shown in Scheme 1, firstly, kanamycin is able to attach onto the surface of AuNPs through electrostatic interactions as well as the interaction between -$NH_2$ of kanamycin and -COOH of the citrate on the AuNPs; then the molecular conformation of glucoside of the kanamycin facilitate the subsequent interaction of kanamycin and AuNPs, changing the surface property of AuNPs, leading to the amounts of •OH radicals and $Au^{3+}$ increased, which induced by reduction and coordination effect. Afterwards, the released •OH radicals participated and accelerated the oxidation of TMB in the presence of $H_2O_2$, the production of $Au^{3+}$ served as strong oxidizing reagent to further improve the oxidation extent of TMB, which in companied with •OH radicals realized the enhancement effects on the AuNPs catalytic activity, made the color of TMB-$H_2O_2$ system changed significantly. As far as we know, this is the first time that systematically investigate the exact process of aminoglycoside antibiotics interact with AuNPs, as well as the effects of simultaneously formation of •OH radicals and $Au^{3+}$ on the peroxidase like properties of Au nanomaterials.

### 3.7. The utility of this method for kanamycin detection in milk and meat

As kanamycin was often used during the process of livestock and poultry husbandry to prevent and cure infections, there is no doubt that kanamycin residues detection in milk and meat is of great significant. To demonstrate the application of our developed method, kanamycin was detected in milk, pork and chicken using AuNPs based colorimetric method and the above-mentioned calibration curve. As

shown in Tables S2-S3, the recoveries were between 98.6–119.5% with the relative standard deviation (RSD) being below 8.4%. In order to show the capacity of the method in the detection of kanamycin in real samples in the presence of other interferences, the real samples (*e.g.*, milk, chicken and pork meat) were detected in the presence of kanamycin and other compounds, as shown in Fig. S15, the absorbance of the solutions in the presence of kanamycin are relatively higher than the solutions in the absence of kanamycin no matter there are other species or not, which indicated that our proposed methods show satisfied specificity in the detection of kanamycin.

In order to show the stability and reliability of this assay, 20 nM and 100 nM kanamycin were added into the milk sample and detected using our proposed method for 7 times in 10 days randomly (no more than one time each day). As shown in Fig. S16. The $OD_{650}$ of solutions in the presence of kanamycin and the calculated concentrations of kanamycin kept constant in 7 days, which demonstrated that our method has good stability and reliability, this may originate from the stability of the citrate-capped AuNPs. These results indicate that our method can be used to determine the amount of kanamycin residues in real samples.

## 4. Conclusions

In summary, we have developed a novel simultaneously enhancement strategy for highly sensitive detection of kanamycin using AuNPs as catalyzer. We demonstrated that the detecting process involved two steps: $-NH_2$ made the kanamycin specially attached on the surface of AuNPs, and the glucoside section of kanamycin further interact with AuNPs, enables the amounts of •OH and $Au^{3+}$ increased in the reaction system, which facilitate the sensitively detect kanamycin with a LOD as 0.1 nM. Compared with previous reported methods, our approach is simple and has reasonable selectivity and enhanced sensitivity. Although kanamycin was chosen here to establish this assay by proof-of-principle experiment, our approach may be transferable to other analytical problems such as the quantitatively determination of pesticide, mycotoxin residues, even microbial contaminations in food, which is meaningful in the food safety management. Further research will focus on the following aspects: using this strategy to detect many other biological molecules; improving the catalytic enhancement effect using other nanomaterials, such as small Au clusters, $CeO_2$ and $Fe_3O_4$ species which possess more active reaction centers; using more technologies to further study the details of interactions between kanamycin and AuNPs. These works are in progress in our lab.

## Acknowledgment

This study was supported by the National Natural Science Foundation of China (No. 21305032), China Postdoctoral Science Foundation (No. 2014M551522), Jiangsu Planned Projects for Postdoctoral Research Funds (1402073B) and the Research Foundation of Jiangsu University (No. 13JDG069).

## Appendix A. Supplementary material

Supplementary data associated with this article can be found in the online version at http://dx.doi.org/10.1016/j.bios.2016.12.042.

## References

Bhattacharya, R., Mukherjee, P., 2008. Adv. Drug Del. Rev. 60 (11), 1289–1306.
Bhattacharjee, M., Pasumarthi, V., Chaudhuri, J., Singh, A.K., Nemade, H., Bandyopadhyay, D., 2016. Nanoscale 8 (11), 6118–6128.
Burns, D.A., Ciurczak, E.W., 2008. Handbook of near-infrared analysis. CRC Press.
Chen, X.W., Hai, X., Wang, J.H., 2016. Anal. Chim. Acta 922, 1–10.
Chen, Y., Wang, Z., Wang, Z., Tang, S., Zhu, Y., Xiao, X., 2008. J. Agric. Food Chem. 56 (9), 2944–2952.
Demers, L.M., Mirkin, C.A., Mucic, R.C., Reynolds, R.A., 3rd, Letsinger, R.L., Elghanian, R., Viswanadham, G., 2000. Anal. Chem. 72 (22), 5535–5541.
Dutta, S., Mandal, N., Bandyopadhyay, D., 2016. Biosens. Bioelectron. 78, 447–453.
Ghosh, P., Han, G., De, M., Kim, C.K., Rotello, V.M., 2008. Adv. Drug Del. Rev. 60 (11), 1307–1315.
Groschel, M., Gotze, R., Muller, S., Ernst, A., Basta, D., 2016. PLoS One 11 (4), 14.
He, J.X., Wang, Y., Zhang, X.Y., 2016. Food Anal. Methods 9 (3), 744–751.
Kim, J.E., Choi, J.H., Colas, M., Kim, D.H., Lee, H., 2016. Biosens. Bioelectron. 80, 543–559.
Kumar, S., Ahlawat, W., Kumar, R., Dilbaghi, N., 2015. Biosens. Bioelectron. 70, 498–503.
Li, B., Du, Y., Li, T., Dong, S., 2009. Anal. Chim. Acta 651 (2), 234–240.
Li, Z., Lei, Z., Wang, Y., Wang, C., Xu, J., Wang, Z., 2014. Anal. Methods 6 (6), 1709–1713.
Lin-Vien, D., Colthup, N.B., Fateley, W.G., Grasselli, J.G., 1991. The Handbook of Infrared and Raman Characteristic Frequencies of Organic Molecules. Academic Press, San Diego, 155–178.
Liu, Y.Y., Wang, G.P., Peng, Z., Guo, J.Y., Wu, Q., Xie, J., Gong, S.S., 2016. Neurosci. Lett. 617, 247–253.
Long, Y.J., Li, Y.F., Liu, Y., Zheng, J.J., Tang, J., Huang, C.Z., 2011. Chem. Commun. (Camb. ) 47 (43), 11939–11941.
Manyanga, V., Dhulipalla, R.L., Hoogmartens, J., Adams, E., 2010. J. Chromatogr. A 1217 (24), 3748–3753.
McCarthy, J.R., Weissleder, R., 2008. Adv. Drug Del. Rev. 60 (11), 1241–1251.
Nie, L., Liu, F., Ma, P., Xiao, X., 2014. J. Biomed. Nanotechnol. 10 (10), 2700–2721.
Oertel, R., Neumeister, V., Kirch, W., 2004. J. Chromatogr. A 1058 (1–2), 197–201.
Patel, K.N., Limgavkar, R.S., Raval, H.G., Patel, K.G., Gandhi, T.R., 2015. J. Liq. Chromatogr. Relat. Technol. 38 (6), 716–721.
Preu, M., Guyot, D., Petz, M., 1998. J. Chromatogr. A 818 (1), 95–108.
Smith, A.M., Duan, H., Mohs, A.M., Nie, S., 2008. Adv. Drug Del. Rev. 60 (11), 1226–1240.
Song, K.M., Cho, M., Jo, H., Min, K., Jeon, S.H., Kim, T., Han, M.S., Ku, J.K., Ban, C., 2011. Anal. Biochem. 415 (2), 175–181.
Strachan, C.R., Davies, J., 2016. J. Ind. Microbiol. Biotechnol. 43 (2–3), 149–153.
Tao, Y., Lin, Y., Ren, J., Qu, X., 2013. Biosens. Bioelectron. 42, 41–46.
Tasho, R.P., Cho, J.Y., 2016. Sci. Total Environ. 563, 366–376.
Wang, C., Dong, X., Liu, Q., Wang, K., 2015. Anal. Chim. Acta 860, 83–88.
Wang, C., Wang, J., Liu, D., Wang, Z., 2010a. Talanta 80 (5), 1626–1631.
Wang, C.K., Chen, D., Wang, Q.Q., Wang, Q.X., 2016. Anal. Sci. 32 (7), 757–762.
Wang, C.K., Liu, D.J., Wang, Z.X., 2011a. Chem. Commun. 47 (33), 9339–9341.
Wang, C.K., Wang, J.E., Liu, D.J., Wang, Z.X., 2010b. Talanta 80 (5), 1626–1631.
Wang, N., Zhu, L., Wang, D., Wang, M., Lin, Z., Tang, H., 2010c. Ultrason. Sonochem. 17 (3), 526–533.
Wang, X.X., Wu, Q., Shan, Z., Huang, Q.M., 2011b. Biosens. Bioelectron. 26 (8), 3614–3619.
Xing, Y.P., Liu, C., Zhou, X.H., Shi, H.C., 2015. Sci. Rep. 5, 8125.
Yildiz, I., 2016. Nanotechnol. Rev. 5 (3), 331–340.
Zhu, R., Zhou, Y., Wang, X.L., Liang, L.P., Long, Y.J., Wang, Q.L., Zhang, H.J., Huang, X.X., Zheng, H.Z., 2013. Talanta 117, 127–132.